Author Manuscript

Author Manuscript

Author Manuscript

Author Manuscript

HHS Public Access

Author manuscript

Nat Chem Biol. Author manuscript; available in PMC 2016 December 20.

Published in final edited form as:

Nat Chem Biol. 2016 August ; 12(8): 614–620. doi:10.1038/nchembio.2106.

Identifying the functional contribution of the defatty-acylase activity of SIRT6

Xiaoyu Zhang[1], **Saba Khan**[1], **Hong Jiang**[1], **Marc A. Antonyak**[2], **Xiao Chen**[1], **Nicole A. Spiegelman**[1], **Jonathan H. Shrimp**[1], **Richard A. Cerione**[1,2], and **Hening Lin**[1,3,*]

[1]Department of Chemistry and Chemical Biology, Cornell University, Ithaca, NY 14853, USA

[2]Department of Molecular Medicine, Cornell University, Ithaca, NY 14853, USA

[3]Howard Hughes Medical Institute, Cornell University, Ithaca, NY 14853, USA

Abstract

Mammalian sirtuin 6 (SIRT6) exhibits many pivotal functions and multiple enzymatic activities, but the contribution of each activity to the various functions is unclear. We identified a SIRT6 G60A mutant that possesses efficient defatty-acylase activity, but has significantly decreased deacetylase activity *in vitro* and no detectable deacetylase activity in cells. The G60A mutant has decreased ability to bind NAD^+, but the presence of fatty-acyl lysine peptides restores NAD^+ binding, explaining the retention of the defatty-acylase activity. Using this mutant, we found that SIRT6's defatty-acylase activity regulates the secretion of numerous proteins. Interestingly, many ribosomal proteins were secreted via exosomes from *Sirt6* KO mouse embryonic fibroblasts, and these exosomes increased NIH 3T3 cell proliferation compared with control exosomes. Our data supports that distinct activities of SIRT6 regulate different pathways, and that the G60A mutant is a useful tool to study the contribution of the defatty-acylase activity to SIRT6's various functions.

INTRODUCTION

Mammalian sirtuin 6 (SIRT6) belongs to the Sir2 (silencing information regulator 2) family of enzymes, which were initially reported as nicotinamide adenine dinucleotide (NAD^+)-dependent protein lysine deacetylases[1]. SIRT6 has attracted a lot of interest because it has pivotal biological functions in regulating genome stability[2,3], DNA repair[4,5], metabolism[6,7], and longevity[8,9]. There are three reported enzymatic activities of SIRT6: deacetylation[3,10–12], defatty-acylation[13,14], and mono-adenosine diphosphate (ADP)-

Users may view, print, copy, and download text and data-mine the content in such documents, for the purposes of academic research, subject always to the full Conditions of use:http://www.nature.com/authors/editorial_policies/license.html#terms

*To whom correspondence should be addressed: Hening Lin, Howard Hughes Medical Institute, Department of Chemistry and Chemical Biology, Cornell University, Ithaca, NY 14853. Telephone number: 607-255-4650. hl379@cornell.edu.

Author Contributions

X.Z. and H.L. designed the research and wrote the manuscript; X.Z. performed all the biochemical and cellular studies except those noted below; S.K. synthesized all the peptides for the *in vitro* deacylation study; H.J. made SIRT6 WT and TNFα plasmids; M.A.A. performed exosome fractionation experiments; X.C. made HEK 293T SIRT6 KO cells; N.A.S. and J.H.S. synthesized Alk14 and BODIPY-N_3; X.Z., R.A.C. and H.L. analyzed the results; H.L. directed all the studies.

Competing Financial Interests Statement

The authors declare no competing financial interests.

Author Manuscript Author Manuscript Author Manuscript Author Manuscript

ribosylation[4,15]. SIRT6 has poor deacetylase activity *in vitro*, but the deacetylase activity can be significantly enhanced by nucleosomes or fatty acids *in vitro*[13,16]. SIRT6 is also reported to exhibit ADP-ribosyltransferase (ART) activity, but this activity is very weak *in vitro*[17] and the physiological relevance of this activity has not been independently validated by other laboratories. We and others have recently identified lysine defatty-acylation as an efficient enzymatic activity of SIRT6[13,14]. *Sirt6* knockout (KO) mice exhibit many phenotypes. They develop lymphopenia, loss of subcutaneous fat, and suffer from severe metabolic defects[2,6]. Now that we know SIRT6 has multiple enzymatic activities, an important question emerges: What is the contribution of each activity to the various functions of SIRT6?

Here we report that a point mutant of SIRT6, Gly60Ala (G60A), maintains efficient defatty-acylase activity but shows no detectable deacetylase activity in cells and no ART activity *in vitro*. Utilizing this G60A mutant, we were able to identify the contribution of defatty-acylation to several functions of SIRT6. We found that the defatty-acylase activity plays little role in regulating gene transcription while it is important for regulating the secretion of many proteins. In particular, in *Sirt6* KO MEFs, many ribosomal proteins were secreted via exosomes and their secretion was blocked by SIRT6 WT or the G60A mutant re-expression. We believe this SIRT6 G60A mutant will be a valuable tool for probing many of the biological functions of SIRT6.

RESULTS

SIRT6 G60A is a lysine defatty-acylase *in vitro*

To find a SIRT6 mutant that only has one of the three catalytic activities, we first tested four reported mutants used in other studies: S56Y, G60A, R65A, and H133Y[4]. S56, G60, R65 are either in or close to the active site of SIRT6, and H133 is the catalytic base necessary for deacylation and is conserved among all seven mammalian sirtuins. It is reported that SIRT6 S56Y and H133Y mutants lack both deacetylase and ART activities, whereas G60A only shows deacetylase activity, and SIRT6 R65A only shows ART activity. We decided to test whether any of these SIRT6 mutants purified from *Escherichia coli* (*E.coli*) showed lysine defatty-acylase activities using a H3K9 myristoyl peptide. One of the mutants, SIRT6 G60A, exhibited approximately 50% of SIRT6 WT defatty-acylase activity, but none of the other three mutants showed defatty-acylase activities (Fig. 1a). We also tested other fatty-acyl peptides (H3K9 palmitoyl, TNFα myristoyl and H3K9 octanoyl), and the results showed that SIRT6 G60A had robust defatty-acylase activities on different peptide substrates (Supplementary Results, Supplementary Fig. 1a–f).

We then tested the deacetylase activities of SIRT6 WT and mutants using a H3K9 acetyl peptide as substrate. We did not observe any deacetylase activity for any of the mutants (Fig. 1b). To ensure that we did not miss any weak deacetylase activity, we added 300 μM palmitic acid in the reactions because it was recently reported that fatty acid can increase SIRT6 deacetylase activity *in vitro*. With 300 μM palmitic acid, 2 μM SIRT6 WT was able to hydrolyze 22% of 25 μM H3K9 acetyl peptide in 2 hours (Fig. 1b). However, SIRT6 G60A only converted approximately 1.8% of H3K9 acetyl peptide to H3K9 peptide, which was close to our HPLC detection limit (Fig. 1b). To further confirm this result, we also purified SIRT6 WT and mutants from HEK293T cells and tested their activities. SIRT6 G60A from

Author Manuscript Author Manuscript Author Manuscript Author Manuscript

HEK293T cells showed comparable defatty-acylase activity with WT (25.6% *versus* 34.8% substrate conversion) but undetectable deacetylase activity (Supplementary Fig. 2a–d).

To make quantitative comparisons, we performed kinetics study for SIRT6 WT and G60A on H3K9 myristoyl and H3K9 acetyl peptides. The k_{cat}/K_m of the demyristoylation activity of SIRT6 WT was 9,100 $M^{-1}s^{-1}$, which was 3.4-fold higher than that of SIRT6 G60A (2,700 $M^{-1}s^{-1}$, Supplementary Table 1 and Supplementary Fig. 3a). The decreased catalytic efficiency was due to decreased k_{cat} (1.9-fold) and increased K_m (1.8-fold). The k_{cat}/K_m of the deacetylation activity of SIRT6 WT was 3.4 $M^{-1}s^{-1}$. This catalytic efficiency is approximately 19-fold better than that of SIRT6 G60A (0.18 $M^{-1}s^{-1}$, Supplementary Table 1 and Supplementary Fig. 3b). When we used 300 μM palmitic acid to activate SIRT6 deacetylase activity, the k_{cat}/K_m for deacetylation of SIRT6 WT was 101 $M^{-1}s^{-1}$, ~30 times faster than that for deacetylation in the absence of palmitic acid (Supplementary Table 1 and Supplementary Fig. 3c). However, 300 μM palmitic acid only increased the k_{cat}/K_m for deacetylation of SIRT6 G60A 3.6 times (0.65 $M^{-1}s^{-1}$, Supplementary Table 1). Therefore, in the presence of 300 μM palmitic acid, the catalytic efficiency of SIRT6 WT deacetylation was approximately 155-fold better than that of SIRT6 G60A.

We then used physiologically relevant substrates of SIRT6, histones, to test the deacetylase activities of SIRT6 WT and mutants. We isolated chromatin fractions from HEK293T cells and incubated with SIRT6 and NAD^+ *in vitro*. SIRT6 WT could almost completely deacetylate histone H3K9 and H3K56, while none of the mutants showed deacetylase activities (Fig. 1c). The deacetylase activity of SIRT6 WT showed dose-dependent effects on H3K9Ac and H3K56Ac while SIRT6 G60A had no activity at any of the concentrations tested (Fig. 1d).

A previous study shows that SIRT6 R65A has ART activity[4]. To confirm that SIRT6 G60A has no ART activity, we tested the ART activities of SIRT6 WT and mutants. SIRT6 WT and R65A showed weak self ADP-ribosylation activities while SIRT6 G60A had no observable ART activity (Supplementary Fig. 4).Therefore, we identified SIRT6 G60A as a mutant with efficient lysine defatty-acylase activity but significantly decreased lysine deacetylase activity on histone peptide, no detectable deacetylase activity on chromatin histones, and no ART activity.

Fatty-acyl peptides promote SIRT6 G60A binding to NAD^+

We next investigated how SIRT6 G60A could maintain defatty-acylase activity but had little deacetylase activity. G60 is on the NAD^+ binding loop (Ala58-Glu75) (Fig. 2a), suggesting that the G60A mutation may change NAD^+ binding affinity. We measured the binding affinities of SIRT6 WT and mutants to NAD^+. SIRT6 contains two tryptophan residues (Trp71 and Trp188) that are close to the active site. It has been reported that SIRT6 tryptophan fluorescence signal decreases after NAD^+ binding[18]. Thus, we determined the dissociation constants (K_d) of SIRT6 WT and mutants for NAD^+ by measuring the tryptophan fluorescence. In the absence of any acyl lysine peptide, the K_d values of SIRT6 WT and H133Y for NAD^+ were 16.7 ± 1.5 μM and 3.2 ± 0.7 μM, respectively (Supplementary Table 2 and Supplementary Fig. 5), which were similar to the reported values[18]. However, the K_d value of SIRT6 G60A for NAD^+ was 564 ± 84 μM

Author Manuscript Author Manuscript Author Manuscript Author Manuscript

(Supplementary Table 2 and Supplementary Fig. 5), suggesting that the G60A mutation significantly decreased NAD^+ binding. We employed another method to confirm that the G60A mutation decreased NAD^+ binding. In this assay, the SIRT6 and NAD^+ solution was filtered with a 10 kDa cutoff membrane. Thus NAD^+ that bound to SIRT6 was retained on the membrane and the unbound NAD^+ would pass through the membrane. When 10 μM SIRT6 WT or the H133Y mutant was incubated with 10 μM NAD^+, 34 ± 3% and 59 ± 3% of NAD^+ were bound to SIRT6, respectively (Supplementary Fig. 6). However, almost no NAD^+ was bound to SIRT6 G60A (2.0 ± 0.7%, Supplementary Fig. 6), again suggesting that SIRT6 G60A bound NAD^+ very weakly.

To probe how SIRT6 G60A could maintain defatty-acylation but had little deacetylase activity, we further measured the binding affinities of SIRT6 WT and G60A for NAD^+ in the presence of acetyl or myristoyl peptides. In the presence of 1 mM H3K9 acetyl peptide, the K_d values of SIRT6 WT or G60A to NAD^+ was 30.3 ± 3.2 μM and 634 ± 91 μM, respectively (Supplementary Table 2 and Supplementary Fig. 5), similar to that without the acetyl peptide. The weak affinity of G60A mutant for NAD^+ in the presence of acetyl peptide explained the significantly decreased deacetylase activity of G60A. We then aimed to measure the binding affinities of SIRT6 WT and G60A for NAD^+ in the presence of the H3K9 myristoyl peptide. However, due to the efficient defatty-acylase activities of SIRT6 WT and G60A, NAD^+ would be consumed quickly in the presence of the myristoyl peptide. Thus we measured NAD^+ kinetics and used the $K_{m,NAD+}$ value to estimate the K_d value. In steady-state, the K_d value is smaller than the K_m value and we can use the K_m value as an upper estimate for the K_d value (Supplementary Fig. 3e). The $K_{m,NAD+}$ value of SIRT6 WT was 33 ± 2 μM (Supplementary Table 3 and Supplementary Fig. 3d), similar to the K_d value of SIRT6 WT for NAD^+ without the myristoyl peptide. Strikingly, the $K_{m,NAD+}$ value of SIRT6 G60A was 47 ± 9 μM (Supplementary Table 3 and Supplementary Fig. 3d), which was much lower than the K_d value of SIRT6 G60A for NAD^+ without the myristoyl peptide. The significantly decreased $K_{m,NAD+}$ value suggested that in the presence of fatty-acyl substrates, SIRT6 G60A could bind NAD^+ tightly and perform defatty-acylation.

Tryptophan fluorescence emission spectra of SIRT6 WT and G60A without any substrate suggested that the G60A mutation changed the conformation of the active site (Fig. 2b). Thermal shift assays revealed that SIRT6 G60A had decreased thermal stability (Fig. 2c). These data suggested that the G60A mutation induces a conformational change that affects SIRT6 stability. The structural changes may affect the NAD^+ binding pocket, leading to loss of NAD^+ binding ability. Furthermore, the altered stability and fluorescence of G60A were not affected by 1 mM H3K9 acetyl peptide (Fig. 2b, c). However, when we added 0.1 mM H3K9 myristoyl peptide, the stability and fluorescence of G60A became similar to those of SIRT6 WT (Fig. 2b, c), suggesting that fatty-acyl substrates could restore the conformation of SIRT6 G60A similar to that of WT and allow SIRT6 G60A to regain high NAD^+ binding ability.

SIRT6 G60A catalyzes only defatty-acylation in cells

We next validated the activity of SIRT6 G60A in cells by detecting the acylation levels of known targets of SIRT6. We chose acetyl-H3K9 and acetyl-H3K56 as cellular readouts for

Author Manuscript Author Manuscript Author Manuscript Author Manuscript

deacetylation since it has been reported that overexpression of flag-tagged SIRT6 is able to decrease acetyl-H3K9 and acetyl-H3K56 levels in 293T cells[19]. We used CRISPR to generate SIRT6 KO in 293T cells (Supplementary Fig. 7) and then overexpressed flag-tagged SIRT6 WT and mutants. Only expression of SIRT6 WT was able to decrease H3K9 and H3K56 acetylation levels (Fig. 3a). The cellular results were therefore consistent with the *in vitro* activity assay results and supported that SIRT6 G60A has no detectable deacetylase activity in cells.

For defatty-acylation, we used TNFα as the cellular readout. We stably expressed SIRT6 WT and the different mutants in *Sirt6* KO mouse embryonic fibroblasts (MEFs) and then transiently transfected TNFα into these cells. The fatty-acylation levels on TNFα were then detected using a fatty acid probe, Alk14, as previously reported[14]. Both SIRT6 WT and G60A expression decreased TNFα lysine fatty-acylation (Fig. 3b), while none of the other mutants did. This result demonstrated that SIRT6 G60A exhibits defatty-acylase activity in cells.

SIRT6 promotes TNFα secretion by defatty-acylation

We previously reported that SIRT6 defatty-acylates TNFα and promotes its secretion. With the G60A mutant available, we further tested whether the defatty-acylase activity of SIRT6 is sufficient for the regulation of TNFα secretion. We stably expressed SIRT6 WT, G60A and H133Y in *Sirt6* KO MEFs and examined TNFα secretion in these cells. SIRT6 WT and G60A expression in *Sirt6* KO MEFs promoted TNFα secretion, while SIRT6 H133Y expression in *Sirt6* KO MEFs had no effect on TNFα secretion (Fig. 3c, Supplementary Fig. 8). These results supported that the regulation of TNFα secretion is achieved through the defatty-acylase activity of SIRT6, which is consistent with our previous report.

SIRT6 suppresses gene transcription by deacetylation

SIRT6 can suppress the transcription activities of various transcription factors, such as NF-κB, HIF1α and c-Myc[6–8]. To investigate whether the defatty-acylase activity of SIRT6 contributes to the transcriptional regulation, we chose several genes (IAP2, GLS, RPL3 and MnSOD) that are known to be regulated by SIRT6 and detected their mRNA levels after overexpression of SIRT6 WT or G60A in *Sirt6* KO MEFs. For all the genes tested, SIRT6 WT overexpression could restore the transcriptional suppression while SIRT6 G60A could not (Fig. 3d, Supplementary Fig. 9). This result suggests that the defatty-acylase activity does not contribute to SIRT6's role in transcriptional regulation of these genes.

It is reported that SIRT6 can suppress glycolysis by inhibiting HIF1α transcriptional activity[7]. Because of the glycolysis suppression function, *Sirt6* KO MEFs are more sensitive to glucose starvation than WT MEFs[6]. Using the sensitivity to glucose starvation, we tested different SIRT6 mutants to find out whether the defatty-acylase activity contributes to this phenotype. SIRT6 WT expression in *Sirt6* KO MEFs rescued glucose starvation-caused cell death, while neither SIRT6 G60A nor H133Y did (Supplementary Fig. 10a, b). Given that SIRT6 G60A has defatty-acylase activity but lacks ART activity and has no detectable deacetylase activity in cells, this result suggests that the defatty-acylase activity is not important for suppressing glucose starvation induced cell death. However, since SIRT6

Author Manuscript Author Manuscript Author Manuscript Author Manuscript

G60A has weaker lysine defatty-acylase activity and lower stability than SIRT6 WT, we could not completely rule out that the failure of SIRT6 G60A to restore this phenotype is due to decreased protein stability or decreased defatty-acylase activity.

SIRT6 regulates the secretion of many proteins

Given that SIRT6 promotes TNFα secretion by defatty-acylation, we wondered whether its defatty-acylase activity regulates the secretion of other proteins. We first detected total secreted proteins in *Sirt6* WT and KO MEFs. As shown in Fig. 4a, the patterns of total secreted proteins in *Sirt6* WT and KO MEFs were different. In contrast, the patterns of total cellular proteins were similar in *Sirt6* WT and KO MEFs (Supplementary Fig. 11). This result suggests that SIRT6 likely regulates the secretion of many proteins.

By performing SILAC (stable isotope labeling with amino acids in cell culture) in *Sirt6* WT and KO MEFs (Supplementary Fig. 12), we identified the secreted proteins that are regulated by SIRT6. We identified 497 secreted proteins with minimal 2 peptides (Supplementary Data Set 1). Among them, 106 proteins showed high (>1.5) Heavy/Light (H/L) ratios, suggesting that SIRT6 decreased the secreted amounts of these proteins, while 117 proteins showed low H/L ratios (<0.667), suggesting SIRT6 increased the secreted amounts of these proteins.

To further confirm that the secreted proteins with high or low H/L ratios were indeed regulated by SIRT6 and to find out which activity of SIRT6 is important for regulating these secreted proteins, we stably expressed SIRT6 WT, G60A, or H133Y in *Sirt6* KO MEFs and performed another three SILAC experiments: SILAC1 was *Sirt6* KO MEFs vs. *Sirt6* KO MEFs expressing SIRT6 WT; SILAC2 was *Sirt6* KO MEFs vs. *Sirt6* KO MEFs expressing SIRT6 G60A; SILAC3 was *Sirt6* KO MEFs vs. *Sirt6* KO MEFs expressing SIRT6 H133Y (Fig. 4b).

We identified 395 proteins with at least 2 peptides detected in all three SILAC experiments (Supplementary Data Sets 2–5). We further filtered the data using the following criteria: H/L ratio in control SILAC3 was close to 1 (0.8–1.25), which served as a quality control as SIRT6 H133Y expression should not change the secreted protein levels. After the filtering, 225 secreted proteins were left. These proteins were further divided into the five groups (Fig. 4b): (1) H/L > 1.5 in both SILAC1 and SILAC2 (50 proteins; SIRT6 defatty-acylase activity decreased the secreted levels of these proteins); (2) H/L < 0.667 in both SILAC1 and SILAC2 (12 proteins; SIRT6 defatty-acylase activity increased the secreted levels of these proteins); (3) H/L > 1.5 in SILAC1, H/L is ~1 (0.8–1.25) in SILAC2 (6 proteins; SIRT6 deacetylase/ART activity decreased the secreted levels of these proteins); (4) H/L < 0.667 in SILAC1, H/L is ~1 (0.8–1.25) in SILAC2 (7 proteins; SIRT6 deacetylase/ART activity increased the secreted levels of these proteins); (5) H/L is ~ 1 (0.8–1.25) in both SILAC1 and SILAC2 (SIRT6 does not regulate the secreted levels of these proteins). Theoretically there should not be proteins that show high H/L ratios in SILAC1 but low H/L ratios in SILAC2 (or vice versa). The analysis of the SILAC data showed that no proteins fell into this category (Fig. 4c). There were 75 proteins in Group 1 to 4 (Supplementary Table 4), suggesting SIRT6 regulates 33% (75 out of 225) of the secreted proteins identified. Datasets of SILAC1 and SILAC2 proteins with altered secretion levels (H/L>1.5 and H/L<0.667)

Author Manuscript Author Manuscript Author Manuscript Author Manuscript

were also analyzed by DAVID Functional Annotation Tool (Supplementary Fig. 13). Based on the datasets analysis, SIRT6 defatty-acylase activity likely regulates pathways involved in ribosome, ECM-receptor interaction, focal adhesion, systemic lupus erythematosus, and cytokine-cytokine receptor interaction, while SIRT6 deacetylase/ART activity likely regulates pathways involved in glycolysis/gluconeogenesis, glutathione metabolism, cysteine and methionine metabolism, and metabolism of xenobiotics by cytochrome P450.

To further validate the SILAC proteomic results for proteins in Group 1 to 4, we chose a few proteins from each group (Supplementary Table 5) and detected their secreted levels and levels in total cell lysates. For Group 1 secreted proteins (RPL17, RPS7, and VCP), the secreted levels were higher in *Sirt6* KO cells than in *Sirt6* WT cells while the levels in total cell lysate were similar (Fig. 5a). Overexpression of SIRT6 WT or G60A mutant in *Sirt6* KO cells decreased the secreted levels to that in *Sirt6* WT cells, suggesting that the defatty-acylase activity of SIRT6 suppresses the secretion of these proteins. We further tested their mRNA levels and found that they were similar with or without SIRT6 (Fig. 5b, Supplementary Fig. 14). These results are consistent with the SILAC data and suggest that SIRT6 defatty-acylase activity suppresses the secretion of these proteins but not the transcription of the corresponding mRNA.

For Group 2 secreted proteins (COL6A1, COL5A1 and CXCL1), the secreted levels were lower in *Sirt6* KO cells than in *Sirt6* WT cells while the levels in total cell lysate were similar (Fig. 5a). Overexpression of SIRT6 WT or the G60A mutant in *Sirt6* KO cells restored the secreted levels to that in *Sirt6* WT cells, suggesting that the defatty-acylase activity of SIRT6 promotes the secretion of these proteins. SIRT6 KO or overexpression did not change their mRNA levels (Fig. 5b, Supplementary Fig. 14), supporting that SIRT6 defatty-acylase activity promotes the secretion of these proteins but not the transcription of the corresponding mRNA. For the secreted proteins in Group 2, we originally thought that SIRT6 may directly defatty-acylate them and promote their secretion, similar to the regulation of TNFα secretion. We tested two of them, COL6A1 and COL5A1, but did not observe any fatty-acylation on these proteins (Supplementary Fig. 15), suggesting that SIRT6 may defatty-acylate other proteins which in turn control the secretion of these proteins.

Although we do not know the exact mechanisms how SIRT6 defatty-acylation regulates the secretion of Group 1 and Group 2 proteins, the sites for this function are likely organelle and plasma membranes. We performed sub-cellular fractionation and imaging experiments and found that overexpressed SIRT6 WT, G60A and H133Y existed in the cytoplasm, nucleus, and membranes (Supplementary Fig. 16). Since protein lipidation is known to mediate membrane association, the defatty-acylation likely take place in organelle membranes or the plasma membrane.

For Group 3 secreted proteins (Annexin A1 and Tenascin), the secreted levels were higher in *Sirt6* KO cells than in *Sirt6* WT cells (Fig. 5a). Different from Group 1 and 2 proteins, the protein levels in total cell lysate were also higher in *Sirt6* KO cells than in *Sirt6* WT cells (Fig. 5a). Only overexpression of SIRT6 WT in *Sirt6* KO cells decreased the secreted levels or the intracellular levels to that in *Sirt6* WT cells, suggesting that the deacetylase/ART

Author Manuscript Author Manuscript Author Manuscript Author Manuscript

activity of SIRT6 suppresses the production of Annexin A1 and Tenascin. This suppression was due to transcriptional regulation of Annexin A1 and Tenascin as the mRNA levels were regulated similarly (Fig. 5b, Supplementary Fig. 14). These results support that SIRT6 deacetylase/ART activity (most likely the deacetylase activity) decreases the secreted levels of Group 3 proteins by suppressing their transcription.

For Group 4 secreted proteins (Rangap1 and Ran), the secreted levels were lower in *Sirt6* KO cells than in *Sirt6* WT cells (Fig. 5a). Surprisingly, the protein levels in total cell lysate and the corresponding mRNA levels were similar (Fig. 5a, b, Supplementary Fig. 14). Only overexpression of SIRT6 WT in *Sirt6* KO cells restored the secreted levels of Rangap1 and Ran to those in *Sirt6* WT cells, suggesting that the deacetylase/ART activity of SIRT6 promotes the secretion of these proteins. This data is consistent with the SILAC result and suggested that SIRT6 promotes the secretion of these proteins post-transcriptionally.

Ribosomal proteins are secreted via exosomes

Among the 50 proteins that are down-regulated by the defatty-acylase activity of SIRT6 (Group 1), 41 are ribosomal proteins, which are not known as classical secreted proteins. We investigated whether these ribosomal proteins were secreted through extracellular vesicles. It is known that SIRT6-deficient cells are tumorigenic[6]. Cancer cells release microvesicles and exosomes to enhance cell-cell communication and deliver oncogenic contents to other cells[20–22]. We isolated microvesicles and exosomes from *Sirt6* KO MEFs that could carry ribosomal proteins (Supplementary Fig. 17a). We used two ribosomal proteins (RPL17 and RPS7) as readout and found that they both existed in exosomes, but not in microvesicles (Fig. 6a). We then validated whether RPL17 and RPS7 secretion via exosomes is regulated by the defatty-acylase activity of SIRT6. We isolated exosomes from *Sirt6* KO MEFs and *Sirt6* KO MFEs expressing SIRT6 WT, G60A, or H133Y. RPL17 and RPS7 can be detected in exosomes from *Sirt6* KO MEFs and *Sirt6* KO MEFs expressing SIRT6 H133Y, but not in exosomes from *Sirt6* KO MEFs expressing SIRT6 WT or G60A mutant (Fig. 6b). This data suggested that SIRT6 defatty-acylase activity inhibits ribosomal protein sorting to the exosomes. We also found that SIRT6 defatty-acylase activity affects many other proteins sorting to the exosomes (Supplementary Fig. 17b).

Sirt6 KO exosomes better promote cell proliferation

We further tested whether the different exosome cargo content could affect the function of exosomes. We isolated the exosomes from *Sirt6* WT MEFs, *Sirt6* KO MEFs, and *Sirt6* KO MEFs expressing SIRT6 WT, G60A, or H133Y, and then treated NIH 3T3 cells with the same number of exosomes. Compared with the cells without exosomes treatment, all exosomes-treated cells showed increased proliferation (Fig. 6c). Particularly, NIH 3T3 cells treated with exosomes from *Sirt6* KO MEFs and *Sirt6* KO MEFs expressing SIRT6 H133Y had significantly higher cell proliferation rate than those treated with exosomes from *Sirt6* WT MEFs and *Sirt6* KO MEFs expressing SIRT6 WT or G60A (Fig. 6c). These results suggested that the exosomes from MEFs lacking SIRT6 defatty-acylase activity had stronger ability to promote cell proliferation, likely due to the different cargo content, such as the ribosomal proteins.

Author Manuscript Author Manuscript Author Manuscript Author Manuscript

DISCUSSION

In this study, we found that the SIRT6 G60A mutant exhibits efficient defatty-acylase activity. Although we observed weak deacetylase activity of SIRT6 G60A on peptide substrate *in vitro* when using high enzyme concentrations, we did not observe any deacetylase activity on chromatin histone H3K9 and K56 *in vitro* or in cells. Our result is, at least in part, different from a previous study that identified SIRT6 G60A originally as a mutant that retained lysine deacetylase activity[4]. The previous report focused on the ART activity of SIRT6 and did not include in-depth quantitative study about deacetylase activity of SIRT6 G60A. It is possible that the deacetylase activity of the G60A mutant in the previous report is also very weak. Alternatively, slight differences in the sequences of the SIRT6 constructs used (e.g. the linker sequences between SIRT6 and the purification tags) may affect the deacetylase activity of the G60A mutant expressed. Luckily for us, our SIRT6 G60A mutant maintains efficient defatty-acylase activity but lack detectable deacetylase activity in cells and therefore is a useful tool to dissect the contribution of defatty-acylation to the various functions of SIRT6.

The unique capability of SIRT6 G60A mutant to remove fatty acyl groups but not acetyl groups can be explained by the fact that the G60A mutation dramatically decreases the NAD^+ binding affinity, but the NAD^+ binding affinity is restored in the presence of fatty-acyl peptides. This is a very interesting phenomenon that presumably originates from the strong binding affinity of fatty-acyl peptides to SIRT6 - part of the binding energy may be used to change the SIRT6 conformation, allowing tight binding of NAD^+.

Using this mutant, we investigated the contribution of the defatty-acylase activity to the biological functions of SIRT6. In the *Sirt6* KO MEFs, if we could restore WT phenotype by expressing SIRT6 G60A, then we interpret that the defatty-acylase activity is important for that phenotype. If only expressing SIRT6 WT could restore the WT phenotype, then we interpret that the defatty-acylase activity is not important and likely the deacetylase or ART activity is important for the phenotype. However, two caveats should be pointed out. First, since SIRT6 G60A showed slightly weaker defatty-acylase activity and lower stability than SIRT6 WT *in vitro*, overexpression of SIRT6 G60A may not be able to restore the function in *Sirt6* KO cells even if that function is regulated by defatty-acylation. Second, for any function that can be restored by expressing SIRT6 G60A, it can be argued that the remaining weak deacetylase activity is sufficient. Nonetheless, based on the test cases with known targets of SIRT6 deacetylation (histone H3 K9 and K56) and defatty-acylation (TNFα), we believe that our interpretations are reasonable.

We found that the defatty-acylase activity of SIRT6 regulates the secretion of numerous proteins. Previously, the only known biological function of the defatty-acylase activity of SIRT6 was to promote TNFα secretion. Thus, our current finding has significantly expanded the role of the defatty-acylase activity of SIRT6. Particularly, many ribosomal proteins are secreted through exosomes in *Sirt6* KO MEFs, and these exosomes can significantly increase NIH 3T3 cell proliferation compared with the exosomes from MEFs expressing SIRT6 WT or G60A. SIRT6 has previously been reported to have tumor suppression function[6]. The proliferation promoting effect of exosomes from *Sirt6* KO cells may partly

Author Manuscript Author Manuscript Author Manuscript Author Manuscript

explain the tumor suppression function of SIRT6. For the secreted proteins in Group 2, we noticed that the secreted levels of many collagens were up-regulated by SIRT6 defatty-acylase activity. Recently it is reported that collagens mediate extracellular matrix remodeling and are important for longevity[23]. Promoting collagen secretion by SIRT6 defatty-acylase activity may be a mechanism underlying the lifespan extension effect of SIRT6 overexpression[9].

As more and more biological functions of SIRT6 are discovered, a fundamental understanding of the role of SIRT6 is getting more desirable. We believe the SIRT6 G60A mutant with efficient defatty-acylase activity but having no detectable deacetylase activity in cells is a useful tool that will provide important insights to help understand the role of SIRT6 in biology.

Online Methods

Reagents

Anti-Flag affinity gel (#A2220) and anti-Flag antibody conjugated with horseradish peroxidase (#A8592) were purchased from Sigma. Human/mouse SIRT6 antibody (#12486), histone H3 (#4499), histone H3K9 acetyl (#9671), histone H3K56 acetyl (#4243), RanGAP1 (#14675), Ran (#4462), Annexin A1 (#8691), Tenascin (#12221), VCP (#2649), HSP90 (#4877), Na,K-ATPase (#3010) and Lamin A/C (#4777) antibodies were purchased from Cell Signaling Technology. β-Actin (sc-4777), GAPDH (sc-20357), COL5A1 (sc-20648) and COL6A1 (sc-20649) antibodies were purchased from Santa Cruz Biotechnology. RPL17 (14121-1-AP) and RPS7 (14491-1-AP) antibodies were purchased from Proteintech. CXCL1 (PA1-29220) antibody was purchased from Thermo Fisher. Brefeldin A, palmitic acid, 3X FLAG peptide, protease inhibitor cocktail, [$^{13}C_6$, $^{15}N_2$]-L-lysine and [$^{13}C_6$, $^{15}N_4$]-L-arginine were purchased from Sigma. Sequencing grade modified trypsin and FuGene 6 transfection reagent were purchased from Promega. ECL plus western blotting detection reagent and universal nuclease for cell lysis were purchased from Thermo Scientific Pierce. Sep-Pak C18 cartridge was purchased from Waters. Amicon Ultra centrifugal filter unit with ultracel-10 membrane was purchased from EMD Millipore. *Sirt6* wild type (WT) and knockout (KO) MEFs were kindly provided by Prof. Raul Mostoslavsky at Massachusetts General Hospital Cancer Center, Harvard Medical School. Acyl peptides (H3K9 acetyl, H3K9 acetyl without tryptophan, H3K9 myristoyl, H3K9 myristoyl without tryptophan, H3K9 palmitoyl, H3K9 octanoyl, TNFα K20 myristoyl and H3K9 free lysine), Alk14, and 6-alkyne-NAD were synthesized according to reported procedures[24–26].

Cell Culture

Sirt6 WT, KO MEFs and *Sirt6* KO MEFs expressing SIRT6 WT, S56Y, G60A, R65A, or H133Y were cultured in Dulbecco's Modified Eagle Medium (DMEM) with 10% heat inactived fetal bovine serum (FBS). Human Embryonic Kidney (HEK) 293T cells and HEK 293T SIRT6 KO cells were cultured in DMEM medium with 10% heat inactived FBS. NIH 3T3 cells were cultured in DMEM medium with 15% heat inactived FBS and MEM non-essential amino acids. All the cell lines have been tested for mycoplasma contamination and showed no mycoplasma contamination.

Author Manuscript Author Manuscript Author Manuscript Author Manuscript

Cloning, expression and purification of SIRT6 WT, S56Y, G60A, R65A and H133Y from *Escherichia coli* (*E.Coli*)

Full-length human SIRT6 was inserted into pET28a vector. SIRT6 S56Y, G60A, R65A and H133Y mutations were made by QuikChange. All the plasmids were transformed into *E.coli* BL21 (DE3) cells and the proteins were purified according to reported procedures[14].

Cloning, expression and purification of SIRT6 WT, S56Y, G60A, R65A and H133Y from HEK 293T cells

Full-length human SIRT6 WT or mutant was inserted into pCMV-Tag 4a vector with C-terminal Flag tag. The SIRT6 WT and different mutant plasmids were transfected into HEK 293T cells using FuGene 6 transfection reagent according to the manufacturer's protocol. pCMV-Tag 4a empty vector was used as negative control. The cells were collected at 500 g for 5 min and then lysed in Nonidet P-40 lysis buffer (25 mM Tris-HCl pH 7.4, 150 mM NaCl, 10% glycerol and 1 % Nonidet P-40) with universal nuclease (1:1000 dilution) and protease inhibitor cocktail (1:100 dilution) at 4 °C for 30 min. After centrifuging at 15,000 g for 15 min, the supernatant was collected and incubated with 20 μL of anti-Flag affinity gel at 4 °C for 2 h. The affinity gel was washed three times with washing buffer (25 mM Tris-HCl pH 7.4, 150 mM NaCl, 0.2% Nonidet P-40) and then eluted by 3X FLAG peptide (dissolved in 25 mM Tris-HCl pH 7.4, 150 mM NaCl and 10% glycerol). Eluted SIRT6 proteins were buffer exchanged three times using Amicon Ultra-0.5 centrifugal filter unit with ultracel-10 membrane. SIRT6 proteins after buffer exchange were used for the deacylation assay.

SIRT6 deacylase activity assay

For the defatty-acylation assay using SIRT6 WT and mutants purified from *E. coli*, 1 μM of SIRT6 WT, S56Y, G60A, R65A or H133Y was incubated in 40 μL of reaction mixture (25 mM Tris-HCl pH 8.0, 50 mM NaCl, 1 mM DTT, 1 mM NAD^+, 25 μM H3K9 myristoyl peptide) at 37 °C for 20 min. For the deacetylation assay (no fatty acid activation) using SIRT6 WT and mutants purified from *E. coli*, 4 μM of SIRT6 WT, S56Y, G60A, R65A or H133Y was incubated in 40 μL of reaction mixture (25 mM Tris-HCl pH 8.0, 50 mM NaCl, 1 mM DTT, 1 mM NAD^+, 25 μM H3K9 acetyl peptide) at 37 °C for 4 hours. For the deacetylation assay (with fatty acid activation) using SIRT6 WT and mutants purified from *E. coli*, 2 μM of SIRT6 WT, S56Y, G60A, R65A or H133Y was incubated in 40 μL of reaction mixture (25 mM Tris-HCl pH 8.0, 50 mM NaCl, 1 mM DTT, 1 mM NAD^+, 25 μM H3K9 acetyl peptide, 300 μM palmitic acid) at 37 °C for 2 hours. To quench the reactions, 40 μL of cold acetonitrile was added into the reaction mixture. After centrifuging at 15,000 g for 15 min, the supernatant was collected and analyzed by HPLC using Kinetex 5u EVO C18 100A column (150 mm × 4.6 mm, Phenomenex). Solvents used for HPLC were water with 0.1% trifluoroacetic acid (solvent A) and acetonitrile with 0.1% trifluoroacetic acid (solvent B). The gradient for HPLC condition: 0% B for 2 min, 0–20% B in 2 min, 20–40% B in 13 min, 40–100% B in 2 min, and then 100% B for 5 min. The flow rate was 0.5 mL/min.

For the defatty-acylation assay using SIRT6 WT and mutants purified from HEK 293T cells, 0.2 μM of SIRT6 WT, S56Y, G60A, R65A or H133Y was incubated in 40 μL of reaction

Author Manuscript Author Manuscript Author Manuscript Author Manuscript

mixture (25 mM Tris-HCl pH 8.0, 50 mM NaCl, 1 mM DTT, 1 mM NAD^+, 5 μM H3K9 myristoyl peptide) at 37 °C for 60 min. For the deacetylation assay using SIRT6 WT and mutants purified from HEK 293T cells, 0.4 μM of SIRT6 WT, S56Y, G60A, R65A or H133Y was incubated in 40 μL of reaction mixture (25 mM Tris-HCl pH 8.0, 50 mM NaCl, 1 mM DTT, 1 mM NAD^+, 5 μM H3K9 acetyl peptide, 300 μM palmitic acid) at 37 °C for 2.5 hours. To quench the reactions, 40 μL of cold acetonitrile was added into the reaction mixture. After centrifuging at 15,000 g for 15 min, the supernatant was collected and analyzed by HPLC using the same method described above.

Kinetics assay for SIRT6 WT and G60A on acetyl and myristoyl peptides

For the demyristoylation kinetics, 0.1 μM of SIRT6 WT or G60A was incubated with different concentrations of H3K9 myristoyl peptides (0.5–64 μM) in 40 μL of reaction mixture (25 mM Tris-HCl pH 8.0, 50 mM NaCl, 1 mM DTT, 1 mM NAD^+) at 37°C for 10 min (SIRT6 WT) or 15 min (SIRT6 G60A). For the deacetylation kinetics without fatty acid, 6 μM of SIRT6 WT or 15 μM of SIRT6 G60A was incubated with different concentrations of H3K9 acetyl peptides (10–320 μM) in 40 μL of reaction mixture (25 mM Tris-HCl pH 8.0, 50 mM NaCl, 1 mM DTT, 1 mM NAD^+) at 37°C for 60 min (SIRT6 WT) or 90 min (SIRT6 G60A). For the deacetylation kinetics with 300 μM palmitic acid, 0.8 μM of SIRT6 WT or 4 μM of SIRT6 G60A was incubated with different concentrations of H3K9 acetyl peptides (5–160 μM) in 40 μL of reaction mixture (25 mM Tris-HCl pH 8.0, 50 mM NaCl, 1 mM DTT, 1 mM NAD^+) at 37°C for 30 min (SIRT6 WT) or 90 min (SIRT6 G60A). To quench the reactions, 40 μL of cold acetonitrile was added into the reaction mixture. After centrifuging at 15,000 g for 15 min, the supernatant was collected and analyzed by HPLC using the same method described above. For all the reactions, the conversions of acyl H3K9 to H3K9 were < 10%.

In vitro histone deacetylation assay

Chromatin was purified from HEK 293T cells. Briefly, the cells were collected at 500 g for 5 min and then lysed in Nonidet P-40 lysis buffer (25 mM Tris-HCl pH 7.4, 150 mM NaCl, 10% glycerol and 1 % Nonidet P-40) with protease inhibitor cocktail (1:100 dilution) at 4 °C for 5 min. After centrifuging at 15,000 g for 5 min, the pellets were collected and washed with the Nonidet P-40 lysis buffer. Then Nonidet P-40 lysis buffer with universal nuclease (1:1000 dilution) and protease inhibitor cocktail (1:100 dilution) were added to the pellets and incubated at 25 °C for 10 min. After centrifuging at 15,000 g for 15 min, the supernatant was collected as chromatin proteins. For the histone deacetylation assay, 1 μM of SIRT6 WT, S56Y, G60A, R65A or H133Y was incubated with 3 μg of chromatin proteins in 30 μL of reaction mixture (25 mM Tris-HCl pH 8.0, 50 mM NaCl, 1 mM DTT, 1 mM NAD^+) at 37 °C for 120 min. Then the SDS loading buffer was added. The whole reaction mixture was heated at 95 °C for 5 min and then used for western blot analysis.

In vitro mono-ADP-ribosylation assay

In vitro mono-ADP-ribosylationassay was performed according to reported procedures[17]. Briefly, 2.5 μM of SIRT6 WT, S56Y, G60A, R65A or H133Y was incubated in 30 μL of reaction mixture (25 mM Tris-HCl pH 8.0, 50 mM NaCl, 1 mM DTT, 50 μM 6-alkyne-NAD) at 30 °C for 30 min. For negative control, 50 μM of NAD^+ was added to replace 6-

Author Manuscript Author Manuscript Author Manuscript Author Manuscript

alkyne-NAD. Then click chemistry was performed. BODIPY-N_3 (1 μL of 4.5 mM solution in DMF), Tris[(1-benzyl-1H-1,2,3-triazol-4-yl)methyl]amine (1.8 μL of 10 mM solution in DMF), CuSO4 (1.5 μL of 40 mM solution in H_2O) and Tris(2-carboxyethyl)phosphine (1.5 μL of 40 mM solution in H_2O) were added into the reaction mixture. The click chemistry reaction was allowed to proceed at room temperature for 30 min. Then SDS loading buffer was added and the mixture was heated at 95 °C for 5 min. The reaction mixture was resolved by 12% SDS-PAGE. Protein gel was incubated in destaining buffer (50% methanol, 40% water, 10% acetic acid) at room temperature for 2 h. BODIPY fluorescence signal was then recorded by Typhoon 9400 Variable Mode Imager (GE Healthcare Life Sciences) with PMT 550 V and normal sensitivity. After recording the fluorescence, the gel was stained by Coomassie blue buffer (0.2% Coomassie brilliant blue R-250 dye, 50% methanol, 40% water, 10% acetic acid) to quantify the protein loading.

Stable overexpression of SIRT6 WT, S56Y, G60A, R65A or H133Y in *Sirt6* KO MEFs

Full-length human SIRT6 WT and mutants were inserted into lentiviral vector (pCDH-CMV-MCS-EF1-Puro) without tag. Lentivirus was generated by co-transfection of SIRT6, pCMV-dR8.2, and pMD2.G into HEK 293T cells. The medium was collected 48 h after transfection and was used to infect *Sirt6* KO MEFs. To obtain the SIRT6 stable overexpressed cells, the cells were treated by 1.5 mg/mL of puromycin 48 h after infection. Empty pCDH vector was used as the negative control.

Detection of lysine fatty-acylation on TNFα by in-gel fluorescence

Human full-length TNFα cDNA with N-terminal Flag tag was inserted into pCMV-Tag 4a vector. The TNFα plasmid was transfected into *Sirt6* KO MEFs and *Sirt6* KO MEFs expressing SIRT6 WT, S56Y, G60A, R65A, or H133Y by FuGene 6 transfection reagent. After 18 h, the cells were treated with 50 μM Alk14 and 4 μg/mL brefeldin A for another 6 h. The cells were collected at 500 g for 5 min and then lysed in Nonidet P-40 lysis buffer (25 mM Tris-HCl pH 7.4, 150 mM NaCl, 10% glycerol, and 1 % Nonidet P-40) with protease inhibitor cocktail (1:100 dilution) at 4 °C for 30 min. After centrifuging at 15,000 g for 15 min, the supernatant was collected and incubated with 20 μL of anti-Flag affinity gel at 4 °C for 2 h. The affinity gel was washed three times with washing buffer (25 mM Tris-HCl pH 7.4, 150 mM NaCl, 0.2% Nonidet P-40) and then re-suspended in 18 μL of washing buffer. BODIPY-N_3 (0.7 μL of 4.5 mM solution in DMF), Tris[(1-benzyl-1H-1,2,3-triazol-4-yl)methyl]amine (1.2 μL of 10 mM solution in DMF), CuSO4 (1 μL of 40 mM solution in H_2O) and Tris(2-carboxyethyl)phosphine (1 μL of 40 mM solution in H_2O) were added into the reaction mixture. The click chemistry reaction was allowed to proceed at room temperature for 30 min. Then SDS loading buffer was added and heated at 95 °C for 10 min. After centrifugation at 15,000 g for 2 min, the supernatant was collected, treated with 400 mM hydroxylamine, and heated at 95 °C for 10 min. The samples were resolved by 12% SDS-PAGE. BODIPY fluorescence signal was recorded by Typhoon 9400 Variable Mode Imager (GE Healthcare Life Sciences) with PMT 550 V and normal sensitivity.

Generation of SIRT6 KO in HEK 293T cells by CRISPR/Cas9 technology

SIRT6 KO HEK 293T cells were generated according to reported procedures[27]. The guide RNAs were cloned into pLKO2 vector. The sequences of guide RNAs are:

Author Manuscript Author Manuscript Author Manuscript Author Manuscript

SIRT6 Nickase pair 3_A: 5'- CACCGTCCATGGTCCAGACTCCGTG-3';

SIRT6 Nickase pair 3_A': 5'- AAACCACGGAGTCTGGACCATGGAC-3';

SIRT6 Nickase pair 3_B: 5'- CACCGACACCACCTTTGAGAGCGCG-3';

SIRT6 Nickase pair 3_B': 5'-AAACCGCGCTCTCAAAGGTGGTGTC-3'.

Western blot

Proteins were resolved by 12% or 15% SDS-PAGE and transferred to polyvinylidene fluoride (PVDF) membrane. The membrane was blocked with 5% BSA in TPBS (0.1% Tween-20 in PBS solution) at room temperature for 60 min. The antibody was diluted with fresh 5% BSA in TPBS (1:5000 dilution for Flag, β-Actin, GAPDH, HSP90, Ac-H3K9, Ac-H3K56 and histone H3, 1:1000 dilution for Na, K, ATPase, Lamin A/C, SIRT6, RanGAP1, Ran, Annexin A1, Tenascin, COL5A1, COL6A1, VCP, RPL17, RPS7 and CXCL1) and then incubated with membrane at room temperature for 1 h (Flag, β-Actin, GAPDH and histone H3) or at 4 °C for 12 h (Ac-H3K9, Ac-H3K56, SIRT6, RanGAP1, Ran, Annexin A1, Tenascin, COL5A1, COL6A1, VCP, RPL17,RPS7, CXCL1, Na, K, ATPase, Lamin A/C and HSP90). For histone H3, Ac-H3K9, Ac-H3K56, SIRT6, RanGAP1, Ran, Annexin A1, Tenascin, COL5A1, COL6A1, VCP, RPL17,RPS7, CXCL1, Na, K, ATPase, Lamin A/C and HSP90 western blots, after washing the membrane three times by TPBS, the secondary antibody (1:3000 dilution in 5% BSA in TPBS) was added and then incubated at room temperature for 1 h. The chemiluminescence signal in membrane was recorded after developing in ECL plus western blotting detection reagents using Typhoon 9400 Variable Mode Imager (GE Healthcare Life Sciences).

ELISA analysis of TNFα secretion in MEFs

After transient transfection of TNFα into *Sirt6* WT MEFs, *Sirt6* KO MEFs and *Sirt6* KO MEFs expressing SIRT6 WT, G60A, or H133Y for 18 h, the medium was changed to fresh medium. The cells were incubated with the new medium for 12 h. Then the medium and the cells were collected separately. Human TNFα ELISA kit (eBioscience) was used for quantifying TNFα in the medium and the cells following the manufacturer's instructions. Percentage of secreted TNFα was calculated by the TNFα in the medium versus total TNFα in the medium and the cells.

Crystal violet assay

The cells were seeded onto 12-well plates at low density (3,000 cells/well). After 48 h, the medium was removed and glucose free DMEM medium with 10% heat inactivated FBS was added into each well for another 72 h. The cells were washed two times with cold PBS, and then fixed with cold methanol for 10 min. After removing the methanol, the crystal violet staining solution (0.2% in 2% ethanol solution) was added and incubated for 5 min. The cells were then washed with water until all excess dye was removed. Crystal violet dye that remained with the cells was solubilized by incubating with 0.5% SDS in 50% ethanol solution. The absorption of crystal violet was measured at 550 nm.

Author Manuscript Author Manuscript Author Manuscript Author Manuscript

Collection of secreted protein in MEFs

The MEFs were cultured to 90% confluence. The medium was removed and the cells were washed 3 times with PBS and then 3 times with serum-free DMEM medium. Then the cells were cultured in serum free DMEM medium for 12 h. The medium was collected and first centrifuged at 500 g for 5 min to pellet floating cells. Then a second centrifugation at 3,000 g for 10 min was carried out to remove cell debris. The supernatant containing total secreted proteins was transferred into Amicon Ultra-15 Centrifugal Filter Units with 10 kDa cutoff for concentration. The concentrated secreted proteins (100–150 times concentrated) were used for SDS-PAGE analysis and Stable Isotope Labeling by Amino acids in Cell culture (SILAC).

SILAC

Sirt6 KO MEFs were cultured in DMEM with [$^{13}C_6$, $^{15}N_2$]-L-lysine and [$^{13}C_6$, $^{15}N_4$]-L-arginine for 5 generations. *Sirt6* WT MEFs, *Sirt6* KO MEFs expressing SIRT6 WT, G60A, or H133Y were cultured in normal DMEM for 5 generations. Then the secreted proteins were collected using the same method described above. After quantifying the concentration of total secreted proteins by Bradford assay, 40 μg of proteins of each pair of samples (heavy labeled and light labeled) was mixed. Disulfide reduction and protein denaturation were performed in 6 M urea, 10 mM DTT, 50 mM Tris-HCl pH 8.0 at room temperature for 1 h. Iodoacetamide was added (final concentration 40 mM) and incubated at room temperature for 1 h. DTT was then added and incubated at room temperature for 1 h to stop alkylation. After diluting the sample 7 times with 50 mM Tris-HCl pH 8.0 and 1 mM $CaCl_2$, trypsin digestion was performed at 37 °C for 18 h. Digestion was quenched with 0.1 % trifluoroacetic acid and the mixture was desalted using Sep-Pak C18 cartridge. The lyophilized peptides were used for LC-MS/MS analysis.

Nano LC-MS/MS analysis

The lyophilized peptides were dissolved in 2% acetonitrile with 0.5% formic acid for nano LC-ESI-MS/MS analysis, which was carried out on a LTQ-Orbitrap Elite mass spectrometer (Thermo Fisher Scientific, San Jose, CA). The Orbitrap was interfaced with Dionex UltiMate3000 MDLC system (Thermo Dionex, Sunnyvale, CA). Protein samples were injected onto a Acclaim PepMap nano Viper C18 trap column (5 μm, 100 μm × 2 cm, Thermo Dionex) at a flow rate of 20 μL/min for on-line desalting and then separated on C18 RP nano column (5 μm, 75 μm × 50 cm, Magic C18, Bruker). The gradient for HPLC condition was 5–38% acetonitrile with 0.1% formic acid in 120 min. The flow rate was 0.3 μL/min. The Orbitrap Elite was operated in positive ion mode with spray voltage 1.6 kV and source temperature 275 °C. Data-dependent acquisition (DDA) mode was used by one precursor ions MS survey scan from m/z 300 to 1800 at resolution 60,000 using FT mass analyzer, followed by up to 10 MS/MS scans at resolution 15,000 on 10 most intensive peaks. All data were acquired in Xcalibur 2.2 operation software (Thermo Fisher Scientific).

RNA extraction, reverse transcription and PCR analysis of the mRNA levels of target genes

Sirt6 WT MEFs, *Sirt6* KO MEFs, *Sirt6* KO MEFs expressing SIRT6 WT, G60A, or H133Y were collected and used for RNA extraction. Total RNAs were extracted using RNeasy Mini

Author Manuscript Author Manuscript Author Manuscript Author Manuscript

kit (QIAGEN). Reverse transcription were performed with SuperScript III First-Strand Synthesis kit (Invitrogen) following the manufacturer's instructions. For PCR amplication, Herculase II Fusion Enzyme with dNTPs Combo kit (Agilent) was used following the manufacturer's instructions. For real-time PCR analysis, iTaq Universal SYBR Green Supermix (Biorad) was used following the manufacturer's instructions. The reaction was monitored using LightCycle 480 II system (Roche).

SIRT6 localization by subcellular fractionation and confocal imaging

Subcellular fractionation and immunofluorescence were performed according to the reported procedures[28,29]. Confocal imaging was performed by Zeiss LSM880 confocal/multiphoton microscope.

Intrinsic tryptophan fluorescence of SIRT6 WT and mutants

Fluorescence emission was monitored by Cary Eclipse Fluorescence Spectrophotometer (Agilent). The excitation wavelength was set as 295 nm (slit 2.5 nm), and the emission spectra were monitored from 320 to 390 nm (slit 5 nm). 3 μM SIRT6 WT, S56Y, G60A, R65A or H133Y in 25 mM Tris-HCl pH 7.4, 150 mM NaCl and 10% glycerol was used for measuring NAD^+ binding. Increasing concentrations of NAD^+ were added to 3 μM SIRT6 WT and mutants solution (0–100 μM NAD^+ for SIRT6 H133Y, 0–500 μM NAD^+ for SIRT6 WT and S56Y, and 0–5 mM NAD^+ for SIRT6 G60A and R65A), and the emission spectra were monitored. To measure SIRT6 WT and G60A binding to NAD^+ with saturated acetyl peptide, 1 mM Ac-H3K9 (without tryptophan) was mixed with 3 μM SIRT6 WT or G60A, then increasing concentrations of NAD^+ were added and the emission spectra were monitored. The peak maximum for each experiment was obtained. The following equation was used for calculating the fraction of NAD^+ bound (*NB*):

$$NB = \frac{F - F_0}{F_{\mathrm{sat}} - F_0}$$

where F is the maximum fluorescence intensity at each NAD^+ concentration, F_0 is the maximum fluorescence intensity with 0 μM of NAD^+, and F_{sat} is the maximum fluorescence intensity with saturated NAD^+. The *NB* values were plotted against NAD^+ concentrations, and the curves were fitted to following equation (one-site binding) using GraphPad Prism:

$$NB = \frac{[E] + [\mathrm{NAD^+}] + K_d - \sqrt{([E] + [\mathrm{NAD^+}] + K_d)^2 - 4 \times [E] \times [\mathrm{NAD^+}]}}{2 \times [E]}$$

where [E] is SIRT6 concentration (3 μM), [NAD^+] is NAD^+ concentration, and K_{d} is the dissociation constant.

To measure the emission spectra of SIRT6 WT and G60A with and without saturated Ac-H3K9 and Myr-H3K9, 3 μM SIRT6 WT or G60A was mixed with 1 mM Ac-H3K9 (without tryptophan) or 0.1 mM Myr-H3K9 (without tryptophan) and then the emission spectra were

Author Manuscript Author Manuscript Author Manuscript Author Manuscript

monitored. The emission spectra of blank buffer and 1 mM Ac-H3K9 or 0.1 mM Myr-H3K9 in blank buffer were also monitored as control.

HPLC analysis of SIRT6 binding to NAD^+

10 μM of SIRT6 WT, G60A or H133Y was incubated with 10 μM NAD^+ in 50 μL of buffer (25 mM Tris-HCl pH 8.0, 50 mM NaCl) at room temperature for 30 min. Then 450 μL of buffer was added and all the 500 μL of buffer with SIRT6 and NAD^+ was transferred to Amicon Ultra-0.5 centrifugal filter unit with ultracel-10 membrane. After centrifuge at 15,000 g for 20 min, all filtrate (~400 μL) was collected and lyophilized. The lyophilized powder was dissolved in 50 μL water and used for HPLC analysis.

Thermal Shift Assay

5 μM of SIRT6 WT or G60A was mixed with or without 1 mM H3K9 acetyl or 100 μM H3K9 myristoyl peptide in the reaction buffer (25 mM Tris-HCl pH 8.0, 50 mM NaCl). The temperature was set from 37 to 62 °C for 3 min in the PCR Thermocycler. Then the samples were centrifuged at 15,000 g for 20 min, the supernatant was analyzed by SDS-PAGE and proteins were visualized by Coomassie blue staining.

Isolation of microvesicles and exosomes

After two 150 mm dishes of the cells grow to 90% confluence, the medium was removed and the cells were washed 3 times with PBS and 3 times with serum-free DMEM medium. Then the culture medium was changed to serum-free medium and the cells were cultured for another 12 h. The medium was collected and subjected to two centrifuges: 500 g for 5 min (to pellet floating cells) and 3,000 g for 20 min (to pellet cell debris). The supernatant was subjected to 0.2 μm syringe filter with low flow rate (<1 drop/second), the vesicles retained on the filter (microvesicles) were washed once by PBS. The microvesicles were then lysed on the filter by Nonidet P-40 lysis buffer (25 mM Tris-HCl pH 7.4, 150 mM NaCl, 10% glycerol, and 1 % Nonidet P-40) with protease inhibitor cocktail (1:100 dilution). The filtrate was subjected to ultracentrifuge at 100,000 g for 2 h. The supernatant was vesicle free medium. The pellets were exosomes and were washed once by PBS and subjected to another ultracentrifuge at 100,000 g for 2 h. To get proteins from the exosomes, the exosome pellets were lysed by Nonidet P-40 lysis buffer (25 mM Tris-HCl pH 7.4, 150 mM NaCl, 10% glycerol, and 1 % Nonidet P-40) with protease inhibitor cocktail (1:100 dilution). For cell proliferation experiment, the exosome pellets were suspended in serum-free DMEM. Exosome concentrations were determined by nanoparticle tracking analysis (NTA) according to the reported procedures[30].

Statistical Analysis

Data were expressed as mean ± s.d. (standard deviation, shown as error bars). Differences were examined by two-tailed Student's *t*-test between two groups; $*p < 0.05$, $**p < 0.01$, $***p < 0.005$.

Supplementary Material

Refer to Web version on PubMed Central for supplementary material.

Author Manuscript Author Manuscript Author Manuscript Author Manuscript

Acknowledgments

This work is supported by a grant from NIH/NIGMS (R01 GM098596). We thank Dr. Raul Mostoslavsky at Massachusetts General Hospital for providing the *Sirt6* WT and KO MEFs, Dr. Peng Chen at Cornell University for the usage of the Fluorescence Spectrophotometer, and Dr. Sheng Zhang at the Proteomic and MS Facility of Cornell University for help with the SILAC experiments performed on a mass spectrometer supported by NIH SIG grant 1S10RR025449-01. Imaging data was acquired in the Cornell BRC-Imaging Facility using the NYSTEM (CO29155)- and NIH (S10OD018516)-funded Zeiss LSM880 confocal/multiphoton microscope.

References

1. Imai S, Armstrong CM, Kaeberlein M, Guarente L. Transcriptional silencing and longevity protein Sir2 is an NAD-dependent histone deacetylase. Nature. 2000; 403:795–800. [PubMed: 10693811]
2. Mostoslavsky R, et al. Genomic instability and aging-like phenotype in the absence of mammalian SIRT6. Cell. 2006; 124:315–329. [PubMed: 16439206]
3. Michishita E, et al. SIRT6 is a histone H3 lysine 9 deacetylase that modulates telomeric chromatin. Nature. 2008; 452:492–496. [PubMed: 18337721]
4. Mao Z, et al. SIRT6 promotes DNA repair under stress by activating PARP1. Science. 2011; 332:1443–1446. [PubMed: 21680843]
5. Kaidi A, Weinert BT, Choudhary C, Jackson SP. Human SIRT6 promotes DNA end resection through CtIP deacetylation. Science. 2010; 329:1348–1353. [PubMed: 20829486]
6. Sebastian C, et al. The histone deacetylase SIRT6 is a tumor suppressor that controls cancer metabolism. Cell. 2012; 151:1185–1199. [PubMed: 23217706]
7. Zhong L, et al. The histone deacetylase Sirt6 regulates glucose homeostasis via Hif1alpha. Cell. 2010; 140:280–293. [PubMed: 20141841]
8. Kawahara TL, et al. SIRT6 links histone H3 lysine 9 deacetylation to NF-kappaB-dependent gene expression and organismal life span. Cell. 2009; 136:62–74. [PubMed: 19135889]
9. Kanfi Y, et al. The sirtuin SIRT6 regulates lifespan in male mice. Nature. 2012; 483:218–221. [PubMed: 22367546]
10. Michishita E, et al. Cell cycle-dependent deacetylation of telomeric histone H3 lysine K56 by human SIRT6. Cell Cycle. 2009; 8:2664–2666. [PubMed: 19625767]
11. Schwer B, et al. Neural sirtuin 6 (Sirt6) ablation attenuates somatic growth and causes obesity. Proc Natl Acad Sci U S A. 2010; 107:21790–21794. [PubMed: 21098266]
12. Yang B, Zwaans BM, Eckersdorff M, Lombard DB. The sirtuin SIRT6 deacetylates H3 K56Ac in vivo to promote genomic stability. Cell Cycle. 2009; 8:2662–2663. [PubMed: 19597350]
13. Feldman JL, Baeza J, Denu JM. Activation of the protein deacetylase SIRT6 by long-chain fatty acids and widespread deacylation by mammalian sirtuins. J Biol Chem. 2013; 288:31350–31356. [PubMed: 24052263]
14. Jiang H, et al. SIRT6 regulates TNF-alpha secretion through hydrolysis of long-chain fatty acyl lysine. Nature. 2013; 496:110–113. [PubMed: 23552949]
15. Liszt G, Ford E, Kurtev M, Guarente L. Mouse Sir2 homolog SIRT6 is a nuclear ADP-ribosyltransferase. J Biol Chem. 2005; 280:21313–21320. [PubMed: 15795229]
16. Gil R, Barth S, Kanfi Y, Cohen HY. SIRT6 exhibits nucleosome-dependent deacetylase activity. Nucleic Acids Res. 2013; 41:8537–8545. [PubMed: 23892288]
17. Du J, Jiang H, Lin H. Investigating the ADP-ribosyltransferase activity of sirtuins with NAD analogues and 32P–NAD. Biochemistry. 2009; 48:2878–2890. [PubMed: 19220062]
18. Pan PW, et al. Structure and biochemical functions of SIRT6. J Biol Chem. 2011; 286:14575–14587. [PubMed: 21362626]
19. Tennen RI, Berber E, Chua KF. Functional dissection of SIRT6: identification of domains that regulate histone deacetylase activity and chromatin localization. Mech Ageing Dev. 2010; 131:185–192. [PubMed: 20117128]
20. Al-Nedawi K, Meehan B, Rak J. Microvesicles: messengers and mediators of tumor progression. Cell Cycle. 2009; 8:2014–2018. [PubMed: 19535896]

Author Manuscript Author Manuscript Author Manuscript Author Manuscript

21. Antonyak MA, et al. Cancer cell-derived microvesicles induce transformation by transferring tissue transglutaminase and fibronectin to recipient cells. Proc Natl Acad Sci U S A. 2011; 108:4852–4857. [PubMed: 21368175]
22. Costa-Silva B, et al. Pancreatic cancer exosomes initiate pre-metastatic niche formation in the liver. Nat Cell Biol. 2015; 17:816–826. [PubMed: 25985394]
23. Ewald CY, Landis JN, Porter Abate J, Murphy CT, Blackwell TK. Dauer-independent insulin/IGF-1-signalling implicates collagen remodelling in longevity. Nature. 2015; 519:97–101. [PubMed: 25517099]
24. Zhu AY, et al. Plasmodium falciparum Sir2A preferentially hydrolyzes medium and long chain fatty acyl lysine. ACS Chem Biol. 2012; 7:155–159. [PubMed: 21992006]
25. Charron G, et al. Robust fluorescent detection of protein fatty-acylation with chemical reporters. J Am Chem Soc. 2009; 131:4967–4975. [PubMed: 19281244]
26. Jiang H, Kim JH, Frizzell KM, Kraus WL, Lin H. Clickable NAD analogues for labeling substrate proteins of poly(ADP-ribose) polymerases. J Am Chem Soc. 2010; 132:9363–9372. [PubMed: 20560583]
27. Cong L, et al. Multiplex genome engineering using CRISPR/Cas systems. Science. 2013; 339:819–823. [PubMed: 23287718]
28. Jedrusik-Bode M, et al. The sirtuin SIRT6 regulates stress granule formation in C. elegans and mammals. J Cell Sci. 2013; 126:5166–5177. [PubMed: 24013546]
29. Huang Z, et al. Tumor suppressor Alpha B-crystallin (CRYAB) associates with the cadherin/catenin adherens junction and impairs NPC progression-associated properties. Oncogene. 2012; 31:3709–3720. [PubMed: 22158051]
30. Soo CY, et al. Nanoparticle tracking analysis monitors microvesicle and exosome secretion from immune cells. Immunology. 2012; 136:192–197. [PubMed: 22348503]

Author Manuscript Author Manuscript Author Manuscript Author Manuscript

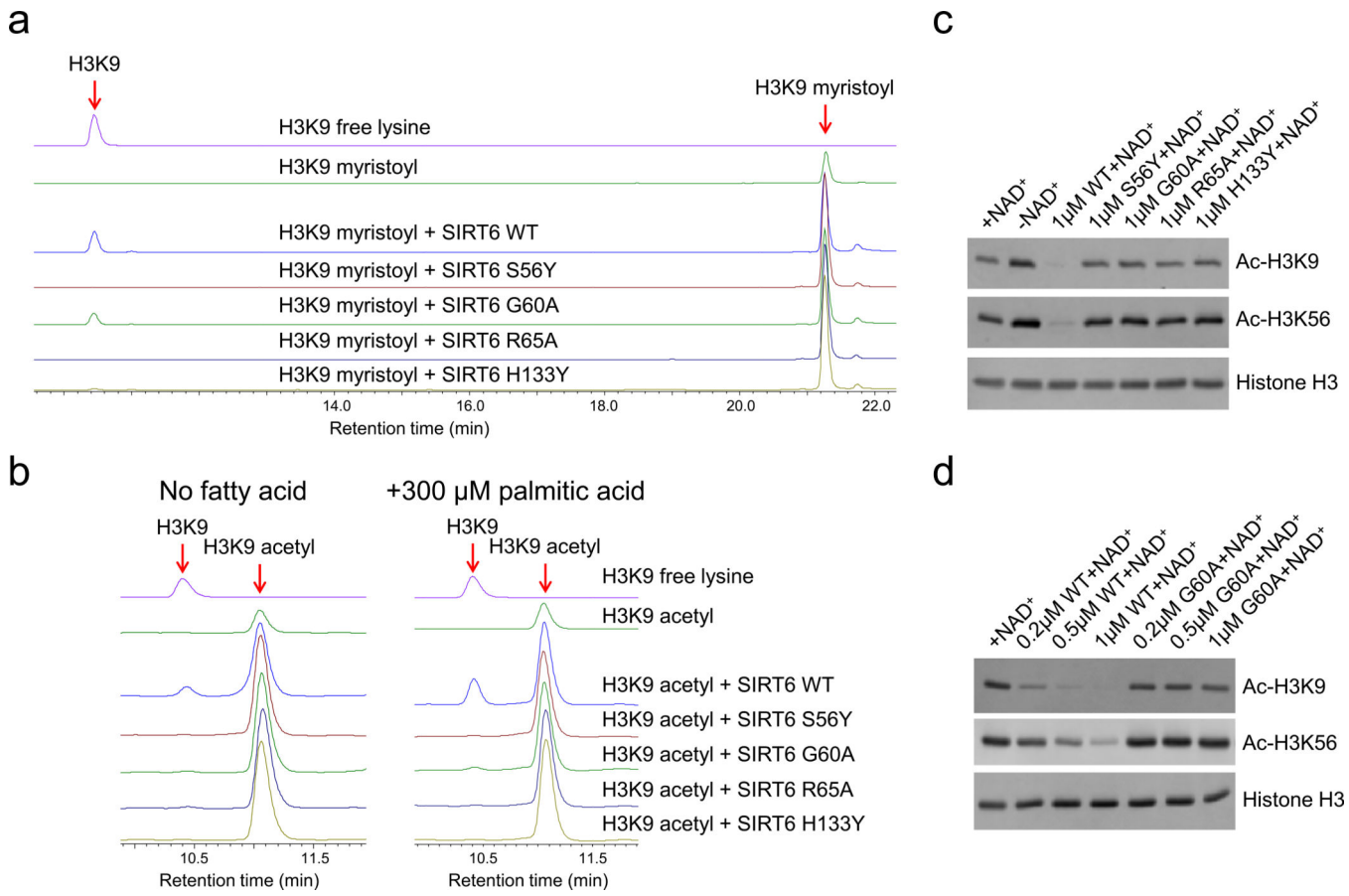

Figure 1. ***In vitro*** **deacetylation and defatty-acylation activities of SIRT6 WT and mutants**

(a) The defatty-acylase activities of SIRT6 WT and mutants analyzed using a H3K9 myristoyl peptide. SIRT6 (1 μM) was incubated with 25 μM Myr-H3K9 and 1 mM NAD^+ at 37°C for 20 min. (b) The deacetylase activities of SIRT6 WT and mutants analyzed using a H3K9 acetyl peptide. SIRT6 (4 μM) was incubated with 25 μM Ac-H3K9 and 1 mM NAD^+ at 37°C for 4 hours (left). Alternatively, 2 μM SIRT6 was incubated with 25 μM Ac-H3K9, 1 mM NAD^+, and 300 μM palmitic acid at 37°C for 2 hours (right). (c) Deacetylation of H3K9 and K56 on chromatin histones by SIRT6 WT and G60A. SIRT6 WT or mutants (1 μM) was incubated with chromatin fractions isolated from HEK293T cells in the presence of 1 mM NAD^+ at 37°C for 120 min. (d) Deacetylation of H3K9 and H3K56 on chromatin histones with different concentrations of SIRT6 WT and G60A. SIRT6 at different concentrations was incubated with chromatin fractions isolated from HEK293T cells in the presence of 1 mM NAD^+ at 37°C for 120 min. Full images of blots in **c** and **d** are shown in Supplementary Fig. 18.

Author Manuscript Author Manuscript Author Manuscript Author Manuscript

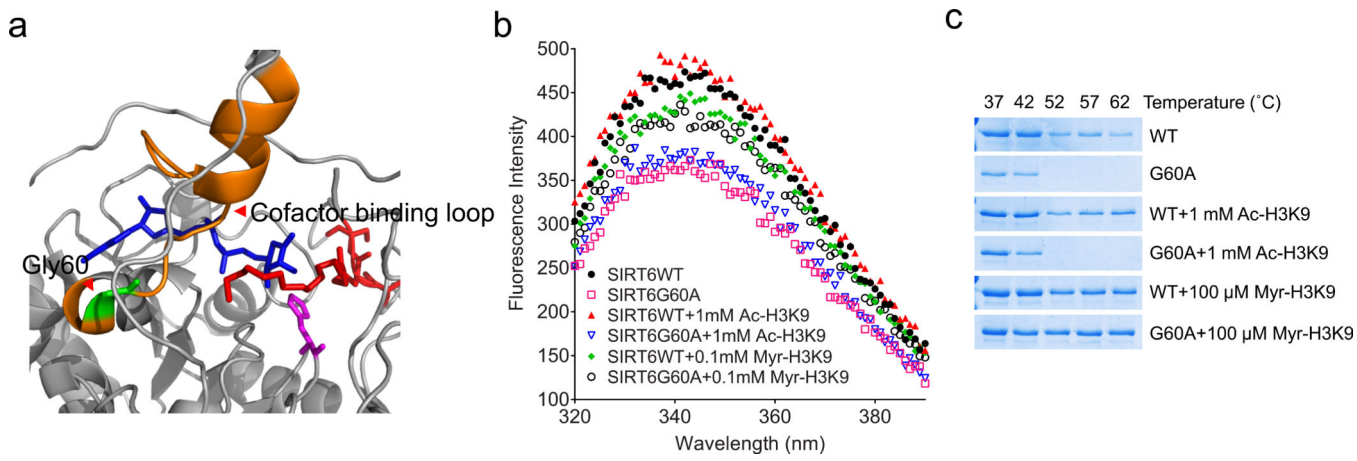

Figure 2. Mechanistic study on how SIRT6 G60A maintains defatty-acylation but loses deacetylation

(a) The location of G60A in the NAD^+ binding loop (Ala58-Glu75) on the crystal structure of SIRT6 (PDB: 3ZG6). (b) Tryptophan fluorescence emission spectra of 3 μM of SIRT6 WT or G60A with or without saturating amount of Ac-H3K9 (1 mM) or Myr-H3K9 (0.1 mM). Each spectrum was repeated three times. (c) Thermal shift assay showing that SIRT6 G60A was stabilized by Myr-H3K9 (0.1 mM) but not by Ac-H3K9 (1 mM). Full images of gels in **c** are shown in Supplementary Fig. 18.

Author Manuscript Author Manuscript Author Manuscript Author Manuscript

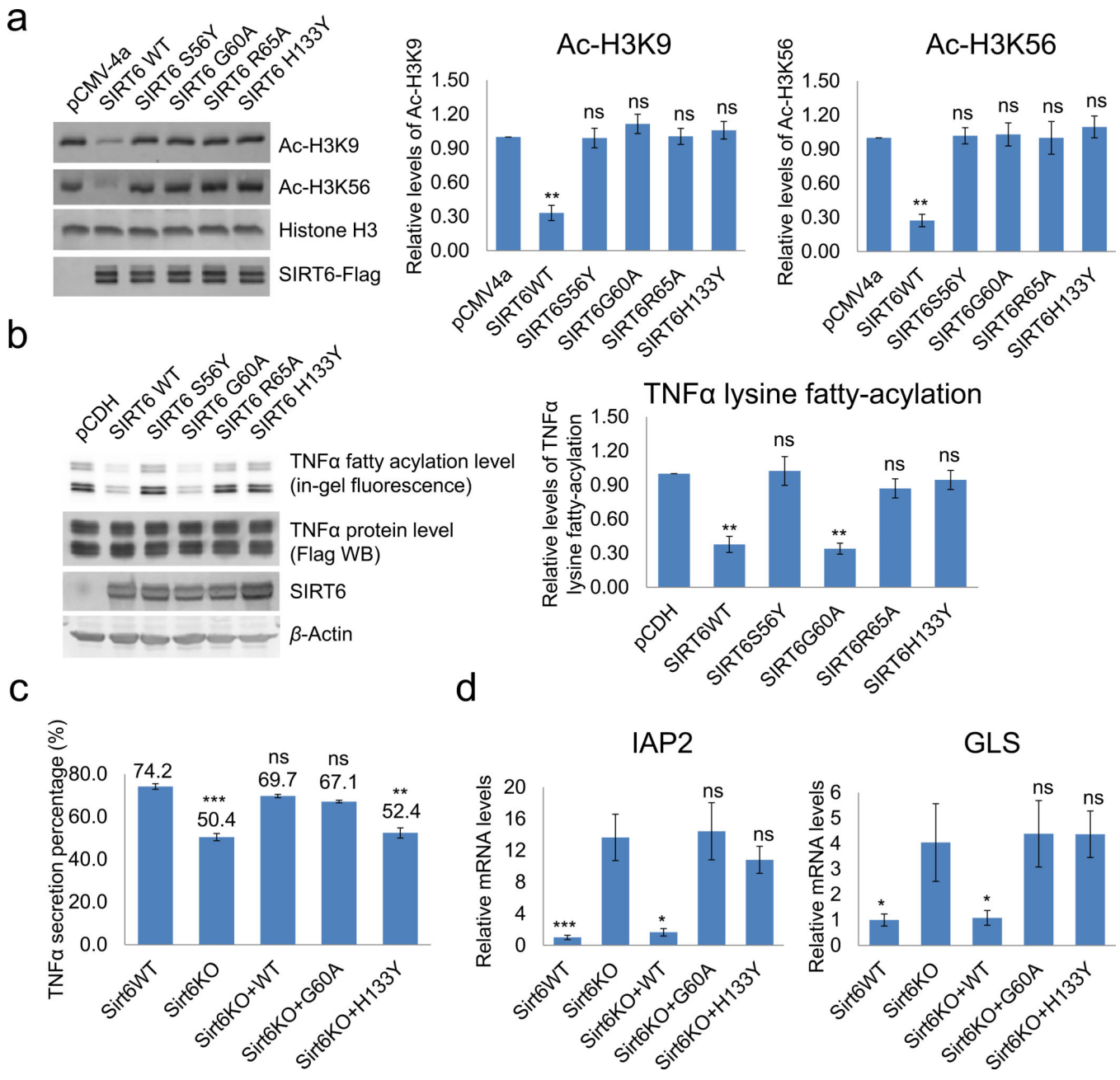

Figure 3. In-cell validation of the deacetylase and defatty-acylase activities of SIRT6 WT and mutants

(a) Left: Western blot analysis of H3K9 and H3K56 acetylation levels in HEK293T *Sirt6* KO cells after transient transfection of SIRT6 WT or mutants. Middle and right: quantification of the Western blot results. Values with error bars indicate mean ± s.d. of three replicates. $^{**}p < 0.01$, for comparing pCMV4a with all the other groups. “ns”, not significant. (b) Left: In-gel fluorescence showing TNFα lysine fatty-acylation levels in *Sirt6* KO MEFs expressing SIRT6 WT or mutants. Right: quantification of the fluorescence gel. Values with error bars indicate mean ± s.d. of three replicates. $^{**}p < 0.01$ for comparing pCDH with all the other groups. (c) Secretion of TNFα in MEFs with or without SIRT6 WT

Author Manuscript Author Manuscript Author Manuscript Author Manuscript

and mutants. Values with error bars indicate mean ± s.d. of three replicates. $^{**}p < 0.01$ and $^{***}p < 0.005$ for comparing SIRT6 WT with all the other groups. (d) Real-time PCR analysis of IAP2 and GLS in MEFs with or without Sirt6WT and mutants. Values with error bars indicate mean ± s.d. of three replicates. $^{*}p < 0.05$ and $^{***}p < 0.005$ for comparing Sirt6KO with all the other groups. Full images of blots and gels in **a** and **b** are shown in Supplementary Fig. 18.

Author Manuscript Author Manuscript Author Manuscript Author Manuscript

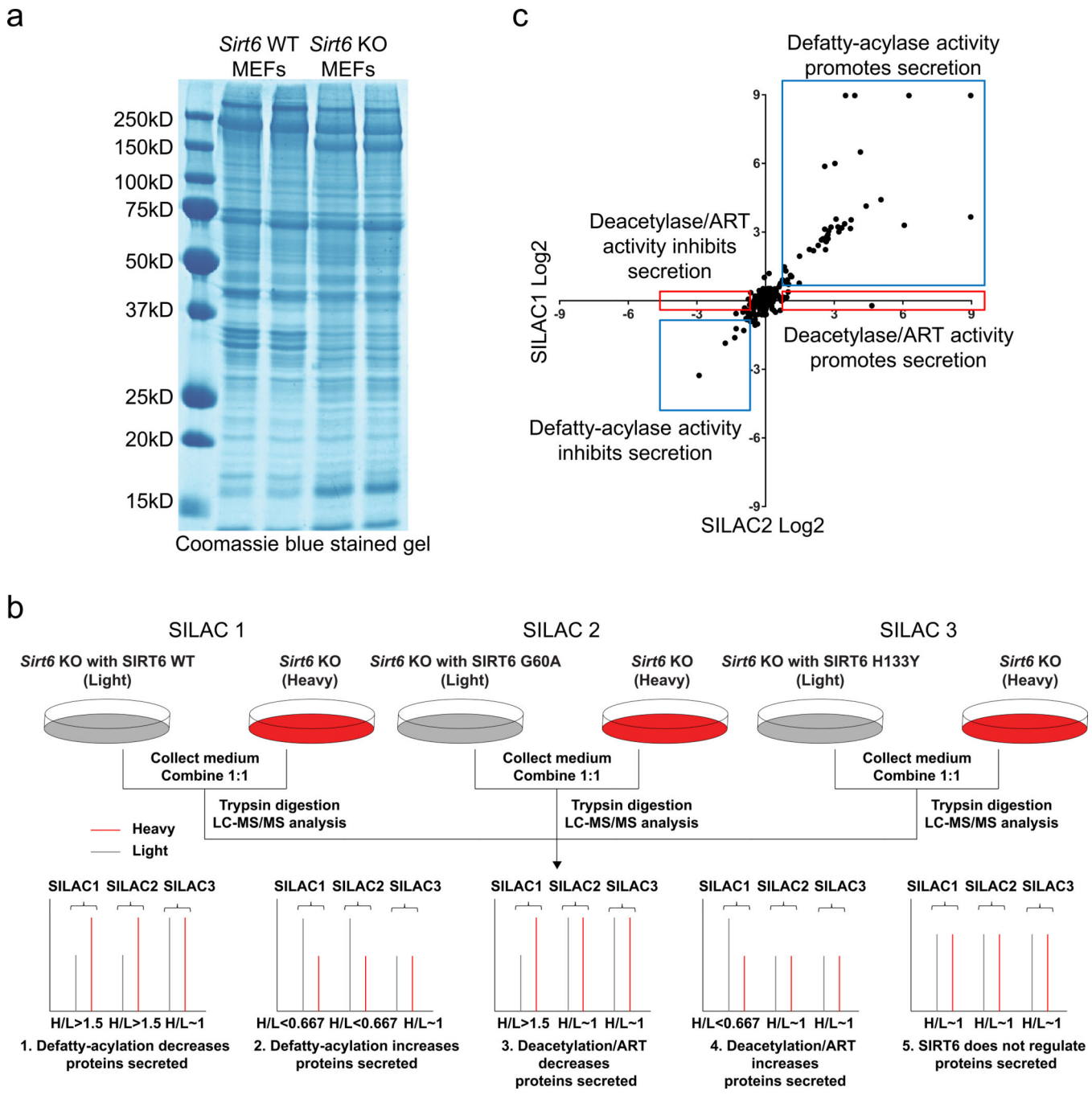

Figure 4. Analysis of secreted proteins by SILAC

(a) The Coomassie blue stained gel of total secreted proteins in *Sirt6* WT and KO MEFs. The two lanes for each cell line were biological replicates. (b) Schematic overview of the SILAC design. (c) Log2-transformation of H/L ratios of proteins identified from SILAC1 (x-axis) and SILAC2 (y-axis) experiments are plotted. Proteins regulated by the defatty-acylase activity of SIRT6 (Group 1 and 2) are in the blue rectangles. Proteins regulated by the deacetylase/ART activity of SIRT6 (Group 3 and 4) are in the red rectangles.

Author Manuscript Author Manuscript Author Manuscript Author Manuscript

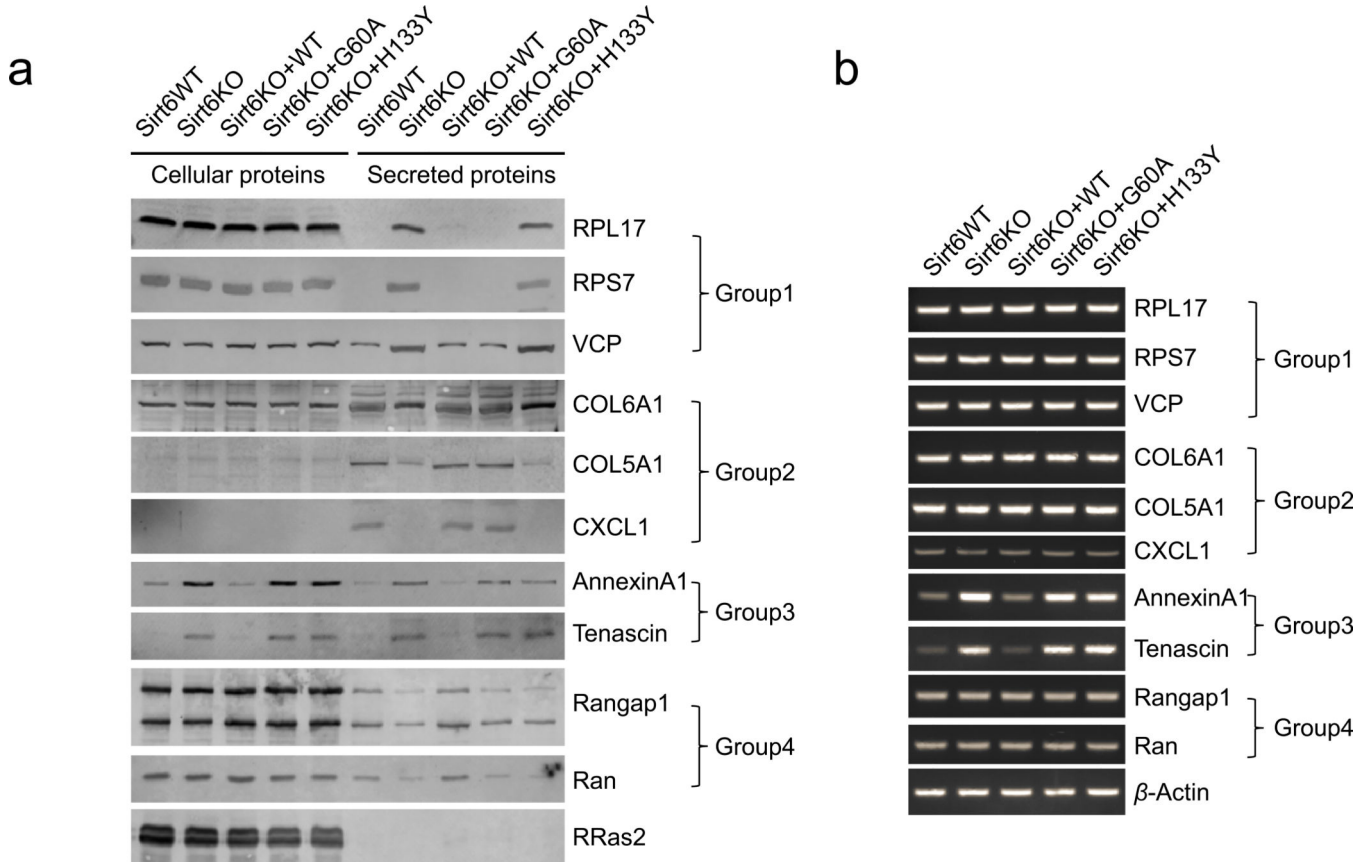

Figure 5. Validation of secreted proteins that are regulated by SIRT6

(a) Intracellular (cell lysates) and extracellular (secreted) levels of representative proteins in different cells. (b) The mRNA levels of representative proteins in *Sirt6* WT MEFs, *Sirt6* KO MEFs, and *Sirt6* KO MEFs expressing SIRT6 WT, G60A, or H133Y. Real-time PCR analysis of the indicated mRNA levels was also done and presented in Supplementary Fig. 12. Full images of blots in **a** are shown in Supplementary Fig. 18.

Author Manuscript Author Manuscript Author Manuscript Author Manuscript

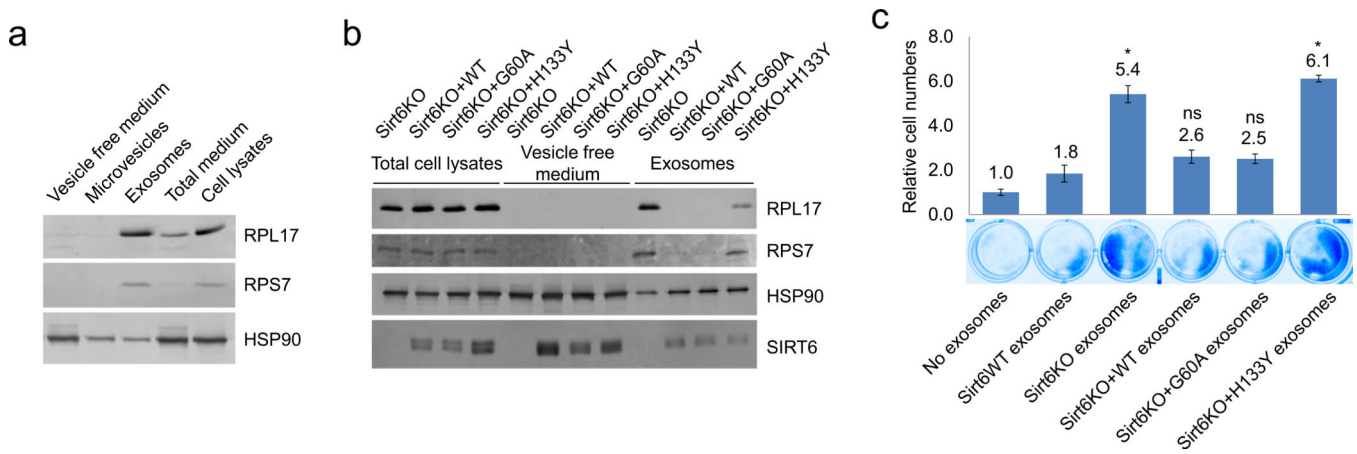

Figure 6. SIRT6 defatty-acylase activity inhibits ribosomal protein sorting to the exosomes

(a) Western blot analysis of RPL17 and RPS7 in different fractions (vesicle free medium, microvesicles, exosomes, and total cell lysates) in *Sirt6* KO MEFs. (b) Western blot analysis of RPL17 and RPS7 in exosomes from *Sirt6* KO MEFs and *Sirt6* KO MEFs expressing SIRT6 WT, G60A, or H133Y. HSP90 was used as the loading control. (c) NIH 3T3 cell proliferation after treating with the same number of exosomes from *Sirt6* WT MEFs, *Sirt6* KO MEFs and *Sirt6* KO MEFs expressing SIRT6 WT, G60A or H133Y. Cell number was determined by crystal violet staining. Error bars indicate mean ± s.d. of three replicates. *$p <$ 0.05 for comparing Sirt6WT exosomes with other exosomes. Full images of blots in **a** and **b** are shown in Supplementary Fig. 18